

Using a Multi-kernel Least Variance Approach to Retrieve and Evaluate Albedo from Limited Bidirectional Measurements

Feng Gao*+, Crystal B. Schaaf*, Alan H. Strahler*, and Wolfgang Lucht‡

* Center for Remote Sensing and Department of Geography, Boston University

+ Nanjing Institute of Geography and Limnology, Chinese Academy of Sciences

‡ Potsdam-Institut für Klimafolgenforschung, Germany

Address correspondence to:

Feng GAO

Department of Geography, Boston University

725 Commonwealth Avenue, Boston, MA 02215

Email: fgao@bu.edu

Tel: 617-353-8033 (O)

Abstract– When a multi-kernel modelling approach is being applied to remotely sensed data, a new criteria - least variance of white-sky albedo - selects semiempirical BRDF kernel combinations better than the more conventional least-squares fitting criteria. The bidirectional reflectance distribution function (BRDF) describes the scattering of light from surface as a function of illumination and view geometry. Semiempirical kernels are nonlinear geometric functions derived from a simplification of physical models of scattering. These are combined linearly to fit observed bidirectional reflectance measurements. White-sky albedo (bihemispherical reflectance) is the integral of directional reflectance for all viewing and illumination directions and is a true surface property. The variance of retrieved white-sky albedo is a function of the noises of measurement, the specific viewing and illumination geometry of the surface scattering measurements, and the number of observations used in the inversion.

By selecting the kernel combination that provides the least variance of white-sky albedo, our studies show that a more stable estimate of white-sky and black-sky (directional-hemispherical) albedo is produced.

INTRODUCTION

Among the BRDF models available, semiempirical models are regarded as some of the most versatile and the easiest to implement. They have the advantage of adjusting to many different kinds of land surface types and can be inverted analytically. These kinds of BRDF models have been widely used for data from the new generation remote sensors such as Moderate Resolution Imaging Spectroradiometer (MODIS) (Justice et al., 1998), Multiangle Imaging Spectroradiometer (MISR) (Diner et al. 1998) and Polarization and Directionality of the Earth's Radiation instrument (POLDER) (Leroy et al., 1997). Both the RossThick-LiSparse-Reciprocal model (Lucht et al., 2000) for MODIS and Roujean's model (Roujean et al., 1992) for POLDER use a simple linear formula of superimposed weighted kernels to describe the bidirectional reflectance as

$$R = C_0 + C_1 K_1 + C_2 K_2. \quad (1)$$

Here R is the modeled value of the bidirectional reflectance, K_1 is the volume scattering kernel, which describes scattering from groundcover layers and is derived from turbid medium theory. K_2 is the surface scattering kernel which simulates the effects of shadowing and is derived from geometrical-optical models. These kernels are physically related to nonlinear functions of the sun-view geometry. C_0 , C_1 , and C_2 are weights for isotropic, volume and surface scattering respectively. Kernel-driven models are regarded as robust BRDF models which can be applied to any kind of earth cover type (Wanner et al., 1995; Strahler et al., 1996; Hu et al., 1997; Privette et al., 1997). The parameters of the linear models are usually easily retrieved by using a least squares method and can be expressed in matrix form

$$\mathbf{m} = [\mathbf{G}^t \mathbf{G}]^{-1} \mathbf{G}^t \mathbf{d} , \quad (2)$$

where

$$\mathbf{G} = \begin{bmatrix} 1 & K_1^1 & K_2^1 \\ 1 & K_1^2 & K_2^2 \\ \dots & \dots & \dots \\ 1 & K_1^n & K_2^n \end{bmatrix} \quad \mathbf{d} = \begin{bmatrix} R_{obs}^1 \\ R_{obs}^2 \\ \dots \\ R_{obs}^n \end{bmatrix} \quad \mathbf{m} = \begin{bmatrix} C_0 \\ C_1 \\ C_2 \end{bmatrix}$$

R_{obs}^i is i th observed bidirectional reflectance. K_1^i is the volume scattering kernel value for the i -th observation geometry. K_2^i the corresponding for surface scattering. The number of total observations is n . The relation between these quantities can be expressed as: $\mathbf{d} = \mathbf{Gm}$.

Studies have revealed that kernel-driven models can be applied to most of the land covers of the earth and can produce a good result when sufficient observations are available (Hu et al., 1997; d'Entremont et al., 1999; Lewis et al., 1997). Hu et al (1997) have shown that certain kernels and kernel combinations best represent certain land cover types (eg., kernels can be somewhat tailored through the use of height and crown shape parameters to better represent tall thin trees or short clumpy shrubs). However this tendency to tie model information to land cover characteristic is only revealed with stable well sampled field data. Since all of the kernels (as well as other semi-empirical and empirical schemes) have been implemented in the kernel-driven BRDF research code (Wanner et al., 1995) (also called Ambrals code which is available from the authors), this modelling framework has been used to explore the relationship between land cover characteristics and albedo in this study. However, a lack of robustness exists when the

kernel selection is performed using a best-fit method due to its strong sensitivity to a small number of large errors in a data set. When limited bidirectional measurements are affected by noise, the kernel combinations that best fit may not actually produce the best results. For instance, when applying the best fit method of kernel selection to NOAA AVHRR data some obviously incorrect white-sky albedos have been obtained. We have analyzed these problematic data sets and found that they contain obviously noisy data.

With the launch of MODIS, MISR, Polder II, and MERIS (Envisat medium Resolution Imaging Spectrometer) we can expect to extract routine global BRDF information confidently from space. In order to obtain enough bidirectional observations to perform a retrieval, a long period of sequential measurement is usually needed to accumulate sufficient observations. While in certain seasons and certain places we can assume that ground covers will not change significantly, it is hard to believe that such a changeable and unpredictable earth will keep in its original state everywhere during multi-week periods. However, if the measurement period is shortened, the number of bidirectional observations available for inversion may decrease. Furthermore, cloud effects will reduce the number of observations. Therefore the number of bi-directional observations available may be limited and therefore, another important issue when using a multi-kernel approach is how to use the best combination of kernels to invert albedo when only a small sample of observations is available. Because of many reasons, such as geolocation, resampling, atmospheric effects etc., our bidirectional reflectance values will always contain a mixture of noise. The final inversion results will include amplified noise which is transferred by an imperfect model from the uncertainty of the measurements. How does this noise and the imperfect model affect the white-sky albedo results and how

is it possible to get a reliable albedo with a small or poor sampling of observations? Those are the questions that are discussed in this paper. This research is part of our continuing study on the use of a variety kernels to best model the data in relation to changing surface conditions – what we call a multi-kernel approach. Note this is in contrast to the stable and robust single kernel combination (RossThick-LiSparse-Reciprocal) approach that is implemented in the at-launch MODIS BRDF/albedo product.

INVERSION METHOD

Before we introduce our inversion method some assumptions need to be stated: all errors from model and noise from measurement are assumed to be Gaussian (Tarantola, 1987). As mentioned, the expression for linear BRDF models is: $\mathbf{d} = \mathbf{G}\mathbf{m}$. According to Tarantola's inverse theory (Tarantola, 1987) the linear inverse problem can be inverted by

$$\mathbf{m} = [\mathbf{G}'\mathbf{C}_D^{-1}\mathbf{G}]^{-1}\mathbf{G}'\mathbf{C}_D^{-1}\mathbf{d} \quad (3)$$

and its covariance matrix is

$$\mathbf{M}_{\text{cov}} = [\mathbf{G}'\mathbf{C}_D^{-1}\mathbf{G}]^{-1}, \quad (4)$$

where the covariance operation \mathbf{C}_D describes uncertainties of the experiment and model. In our inversion, the covariance matrix is determined by the uncertainties of measurements, the errors of the model and the bidirectional geometries of measurements. In formula (4) the covariance matrix of parameters is only related to the sampling position, kernels and the precision of measurements. They are independent on the value

of bidirectional reflectance. The bihemispherical integrals of the BRDF model kernels over view and solar hemispherical space can be written as

$$H_k = \frac{2}{\pi} \int_0^{\frac{\pi}{2}} \int_0^{2\pi} \int_0^{\frac{\pi}{2}} (K_k(\theta_i, \theta_v, \phi) \sin \theta_v \cos \theta_v \sin \theta_i \cos \theta_i) d\theta_v d\phi d\theta_i \quad (5)$$

The bihemispherical reflectance (white-sky albedo) can be simplified as a sum of linear weights: $\rho_w = \sum_k m_k H_k = \mathbf{w}' \mathbf{m}$. Here \mathbf{w} is the vector of H_k . They can be calculated independently and used as look up tables (Strahler et al., 1996). The variance of the white-sky albedo can be calculated by

$$\sigma_{\rho_w}^2 = \mathbf{w}' * \mathbf{M}_{\text{cov}} * \mathbf{w} \quad (6)$$

If the covariance \mathbf{C}_D which describes uncertainties of the experiment and model can be simplified as $\mathbf{C}_D = \sigma_D^2 \cdot \mathbf{I}$, where σ_D^2 is the estimated equal variance of measurement and model, \mathbf{I} is the unit matrix, (i.e., the uncertainties in the observations are independent and have equal magnitude), then formula (3) can be simplified to formula (2) and it follows that:

$$\sigma_{\rho_w}^2 = \sigma_D^2 \mathbf{w}' [\mathbf{G}' \mathbf{G}]^{-1} \mathbf{w} \quad (7)$$

That means that once the kernel-driven BRDF models are specified and errors of measurement are assumed the same, the inversion results derived by the least square method and by Tarantola's inverse theory are the same. In formula (6), the variance of white-sky albedo only depends on the BRDF kernels, bidirectional observation position and errors of measurement and does not depend on the reflectance itself. It can be thought of as a noise amplifier spreading from the measurements to the white-sky albedo through the kernels.

In the selection of different kernels to compose a BRDF model, the simplest method is to select kernel combinations which can create the best fit result for the measurements and this method has been used in the kernels-driven BRDF model (the Ambrals model) and has been described in Wanner et al. (1995). If a lot of observations are available, this method can produce good results. But instead of selecting kernels which best fit the measurements but may result in an albedo with larger variance, we put forward a new criteria, which called the least variance method, which will select the kernel combinations yielding the least variance of white-sky albedo. Since kernels yielding the least variance of white-sky albedo will have the least sensitivity to noise from measurements, the inversion results of white-sky albedo are more reliable. Since we haven't the knowledge to determine the uncertainty of each bi-directional measurement, we assumed the uncertainties in the observations are independent and have equal magnitude in the following investigation of the new method. As we mentioned above, the inversion results which are calculated by the least square method and Tarantola's inversion theory are the same for a certain kernel-driven BRDF model under this assumption. However, the fitting errors and variances of white-sky albedo will change for the different kernel-driven BRDF models. The usual method is to pick a kernel-driven BRDF model which has the smallest fitting errors. The new method is to pick a kernel-driven BRDF model which has the smallest variance of the white-sky albedo. In our new approach, if errors of measurement for different bands are assumed linear, the variance of white-sky albedo for different bands will keep the same linear relationship and the selected kernel-driven model will be same for all bands. Kernels selected by the least variance method will be the same for all bands under the assumption that errors of

measurement among all bands have a linear relationship. Therefore it can be a band-independent method. The variance of white-sky albedo also depend on the numbers of terms in the kernel-driven BRDF model. In this study, we always used all 3 terms (isotropic, volumetric and geometric terms) in the model. The least variance method is not suitable for the selection of models with different terms.

When errors of measurement can be estimated, the variance of white-sky albedo given by formula (6) can provide us a quality assessment of white-sky albedo and help us to determine whether we would like to use this result. The determination created by the least variance of white-sky albedo is a more robust criteria than that of merely specifying a number of clear looks. This is because sometimes fewer looks may actually include more information and yield a smaller variance of white-sky albedo, resulting in a white-sky albedo that is more reliable than that of an albedo based on more looks.

EVALUATION OF THE LEAST VARIANCE METHOD

General Tests

Five different BRDF measurements collected by Kimes (1983) were used in this test. They are field, hardwood, pine, soybean, and grass. These were selected to represent different basic types of land surfaces (barren, broadleaf and needleleaf trees, broadleaf and grass-like herbaceous plants). Each of the measurement sets was then sampled into 5 groups. Group (A) includes all original observations. Other groups are subsets of the group (A). All 6 observations in the group (B) are in the near-nadir direction and there is an absence of observations with large view zenith angles. Compared to group (B), group

(C) includes one more observation with a large view zenith angle. It therefore contains more information than group (B). Observations in the group (D) are sparsely but well sampled over the whole hemisphere of the BRDF. It includes 6 observations. Group (E) include only three observations in the principal plane, which is the least number of observations possible for the full inversion of three parameters models. Figure 1 shows the position of those five data sets in the sphere space.

Fig. 1 Test data sets (B)-(E) were deliberately selected from data set (A) and were prepared to be used in testing two inversion methods.

In the family of kernels considered in the multi-kernel approach, the selectable volume scattering kernels include RossThick and RossThin. The selectable surface scattering kernels include Roujean, LiDenseLO, LiDenseLP, LiDenseHO, LiDenseHP, LiDenseModis, LiSparseLO, LiSparseLP, LiSparseHO, LiSparseHp, LiSparseModis. Those kernels were defined by Roujean et al. (1992) and Wanner et al. (1995). The Li series of kernels were then revised to reciprocity (Lucht, 1998). All of the kernels used in this paper are reciprocal, i.e., sun and viewing angle are exchangeable. RossThin and RossThick describe small and large values of the leaf area index. LiDense and LiSparse describe dense and sparse canopy. The trees (or objects) are modeled as spheroids with vertical radius b , horizontal radius r , and height to the center of the crown h . The surface kernels can be expressed as different surface types which have different ratio of b/r and h/b describing crown shape and relative height, which were called LO, LP, HO, HP, Modis. (The values chosen are $b/r = 0.75$ and $b/r = 2.5$ for crown shape, representing a slightly oblate (O), still rather round crown, and a prolate (P) crown; the values chosen

for relative height are $h/b = 1.5$ and $h/b = 2.5$, representing a low (L) and a high (H) case. Modis is a extra case with $b/r = 1$ and $h/b = 2$). The recent implementation of the RossThick-LiSparse-Reciprocal kernel in MODTRAN 4 will allow the user to attempt different ratios of b/r and h/b although the documentation warns the user not to be too literal in this interpretation due to the correlation between kernels which occurs because of multiple scale interactions (Acharya et al., 1999). Table I shows the inversion results of the best-fit method and the least variance method. The uncertainties of reflectance for all observations were set to 0.1 and covariance of different observations were set to 0 in all data sets. Although we haven't an independent verified measurement of the true albedo, group A (since it includes the most observations) was regarded as the more accurate value. The albedos derived by the best-fit approach and the least variance approach in group A are very similar. Group B includes less information because the observations are clustered near nadir and there is no information about observations with large view zenith angles. With this very poor sample, most of the results of the white-sky albedo created by the best-fit method are obviously wrong. They are very sensitive to the noisiness of the reflectances because their standard deviations are much bigger than the uncertainties of the observations. The inversion results are very unstable even though the sum square of errors reached a minimum value. Still, by using the data in group B, the least variance method yielded more reasonable results although not necessarily very accurate either. The standard deviations of white-sky albedo are much smaller than those derived by the best-fit method. The result is more reliable even though its sum square of errors are not minimal. Some white-sky albedos produced by the best fit method even go to negative because of the failed inversion of BRDF model. By adding some information

to group B, we created group C which includes a single additional large view zenith observation besides the data present in group B. Some results, such as hardwood, derived by the best fit method are not improved even though group C included more information. In group B, the best-fit method and the least variance method both happened to select the same kernels in the red band and got a smaller standard deviation of white-sky albedo. But in group C different kernels were selected by the two methods. We obtained a larger standard deviation of white-sky albedo and also a less appropriate white-sky albedo value with the minimal least squares error best-fit method than the least variance method. However, even the white-sky albedo derived by the least variance method in group C is not as good as it was in group B (in comparison with the results of group A). The reason is that the one additional observation is probably more noisy although we still assumed the noise effects were the same for all observations. It has important contribution to the BRDF shape and changed the white-sky albedo. The standard deviation of white-sky albedo is not only dependent on the number of looks, the geometries of looks, the BRDF models, but also dependent on the uncertainty of the measurements which is more difficult to quantify. Observations in the group D were distributed over the whole hemisphere. They included more information about BRDF shape than group B and group C. Both of the two selection methods produced good results. The standard deviations of white-sky albedo decreased. From their standard deviations we can deduce that group D includes more information than group C. The data in group E only includes 3 observations. Since the sum of squares of errors of all of the kernel combinations were zero, the best fit method failed and it is impossible to distinguish which combination is better. But standard deviations of white-sky albedo are different. Therefore we can select

the best solution by the least variance method. The inversion results of group E by the least variance method look good. It is even better than some results in the group B and group C which were derived by the best fit method and have a smaller standard deviations. From their standard deviations we can deduce that group (A) of course includes more BRDF information than group (D), which contains more than group (C), which contains more than group (E), which finally contains more than group (B). In this example, group (E) includes more information than group (B) even though group (B) has more observations. This general tests show the least variance method is more robust than the best-fit method of kernel selection while being applied to the poor data set. Observations with fewer looks may actually include more BRDF information than those with more looks. More statistical results will be discussed in the following sections.

Table 1 Inverted results of two methods

Since remotely sensed measurements contain noise and a BRDF model is always an approximation of the real world, the minimal least squares error best fit method of kernel selection does not always produce the best albedo. The least variance method can deal with noise from both the measurement and the model and always selects the kernel combinations with the least sensitivity to noise. Therefore least variance produces a better result when only a small number of observations are available. The variance of white-sky albedo can help us to understand our measurements and results. It is a better indication of how much confidence we can place on the albedos retrieved regardless of the number of looks and it can be used in product quality assessment. It is important to note that this has

nothing to do with the principal ability of the kernel models to correctly model albedo. The least variance inversions are based upon the very same models as are the least squares inversions. Where sampling is sparse, however, the criterion of least squares does not serve well in the selection of kernels and associated parameters, and hence may lead to unreliable results. The least variance criterion is the better criterion for model selection and inversion.

Capacity to Interpolate and Extrapolate

Six land cover types measured by the PARABOLA radiometer were chosen for testing the capacities of these two kernel selection methods to interpolate and extrapolate. They are soil, grass, cotton, aspen, black spruce and jack pine. The canopy LAI values, number of solar zenith angles and white-sky albedos calculated from the original measurements are listed in table 2 (values taken from Privette et al., 1997). The reason we used PARABOLA measurements here is because they provide more observations at different solar zenith angles.

Table 2 Six land cover types selected for testing the capacities of interpolation and extrapolation

For black-sky albedo, the capacity of interpolation was defined as an ability to predict black-sky albedo at a solar zenith angle similar to that under which the measurements were made. The capacity of extrapolation was defined as an ability to predict black-sky albedo at different solar zenith angles. In this test, we first created a MODIS-like data set from the measurement. The MODIS-like data were chosen from the

measurements which have the most similar geometry to the MODIS-AM observations. First we used the orbital simulation software Xsatview (Barnsley et al., 1994) to create MODIS observation geometries for the whole globe and a whole year, then selected the continuous 16 days of cumulative observation geometries from MODIS-AM which had the most similar solar zenith angle to measurement. Finally, we used those 16-day observation geometries to find corresponding observations from the PARABOLA measurement. Those 16 continuous days worth of observations were then randomly subsetted to create 65 data sets which had a number of looks varying from 4 to 16. Table 3 lists the percentage relative errors of interpolation and extrapolation for black-sky albedo in the red and the NIR bands. They are the averages of the 65 data subsets. The “real values” of black-sky albedo were derived from all of the observations of the original measurement by

$$\rho_{SZA} = \frac{\sum R_{SZA}^i \cdot \sin \theta_v^i \cdot \cos \theta_v^i}{\sum \sin \theta_v^i \cdot \cos \theta_v^i}, \quad (7)$$

where i is i -th observation at solar zenith angle SZA . R_{SZA}^i is the bi-directional reflectance at solar zenith angle SZA . θ_v^i is viewing zenith angle.

From table 3 we can see that all but three of the relative errors of black-sky albedo derived by the least variance method are smaller than those of the best-fit approach. Therefore the least variance method of kernel selection selects models with better capacities to interpolate and extrapolate than the best-fit method.

Table 3 Relative interpolated and extrapolated errors of black-sky albedo derived by the least variance and by the best-fit methods in red and in the NIR band.

Angular Sampling Dependence

One of the big effects on BRDF inversion is the geometry of the sampling. Angular sampling may be poor due to cloudiness or sensor characteristics. In this test, we used several kind of land covers including field, grass, pine, hardwood, and soybean collected by Kimes (1983) and inverted for albedo using small randomly selected subsamples of the observations. Figure 2 shows white sky albedos inverted by the best-fit method and by the least variance method with only 4 observations. Those data subsets with 4 observations were randomly selected from the full data sets. The two respective albedos are shown as a scatter plot as in Figures 2a and 2b. From the Figure 2, one can see that albedos inverted by the best-fit method are more varied than those found from the least variance method. They are therefore more sensitive to variations in the bidirectional observation geometries.

Fig. 2 Retrieved albedos may be affected by variations in the geometries of the observations.

Sensitivity to Sampling Size

When the number of observations increases, the deviation of inverted albedos from the true value will decrease. Figure 3 shows the change of standard deviation with the increase of the numbers of observations for both the best-fit and the least variance methods. Note that the total number of observations is less than 10 even for the best-sampled case, as is realistic for polar-orbiting cross-track scanning satellite observations

in a 2-3 week period. For each number of observations obtained, bidirectional reflectance was randomly selected from the original whole data set and albedo were calculated. The process was repeated 100 times for each number of observations. The mean values of white-sky albedo and their standard deviation were calculated.

Fig. 3 The accuracy of retrieved albedo may be affected by the number of looks available.

From the figure, one can see that as the number of observations decreases, the standard deviation of white-sky albedo derived from the minimal least squared error best-fit method of model selection increased faster than that from the least variance method. For each sample size the standard deviation of white-sky albedo derived from the least variance is always smaller than that from the best fit method. Even when the number of observations is as small as 3 the inversion results obtained using the least variance method are still as stable as those obtained with the best fit method for 8 observations. This shows that the least variance method is less sensitive to the sampling size and the result are hence more stable.

Application to New England AVHRR Data

By using the least variance method we computed an albedo map of New England using AVHRR data which had been processed in a manner described by d'Entremont et al (1999). The bidirectional reflectances were extracted from NOAA AVHRR images for

a 16-day time period in September, 1995. The images were calibrated, geolocated and carefully cloud-cleared. They have a nominal spatial resolution of 1km (d'Entremont et al., 1999). Figure 4a shows the inversion results for the NIR white-sky albedo obtained by the least variance method of kernel selection. Black area is water or those pixels which can't be inverted because of a lack of observations (pixels which have 3 or more looks are inverted in this map). Figure 4b shows the NIR white-sky albedo inversion results by the best-fit method of kernel selection. Pixels which have 4 or more looks (which is the smallest number of looks possible for the best-fit method) are inverted in this map. Comparing 4a and 4b, we find that Figure 4a shows very good geomorphic features (valleys, forests, and urban areas) while Figure 4b is more noisy. Figure 4c is the map of standard deviation of white-sky albedo. The errors of measurement and model were set to 0.1. Figure 4d is a map of the number of clear looks. While we can see some relationships between Figures 4c and 4d because the number of clear looks obviously directly affects the variance of white-sky albedo, there are some obvious differences between these figures, which is caused by the different bidirectional geometry of the observations. Some measurements with fewer looks may include more information than measurement sets with more looks. The standard deviation of white-sky albedo can be used as a judgment of product quality. Figure 4c can help us to understand the albedo map and to decide which pixels cannot be used with confidence.

Fig. 4 NIR band albedo of New England derived using the least variance method from NOAA AVHRR data for a time period in September, 1995. (a) albedo map by the least

variance method, (b) albedo map by the best-fit method, (c) variance of albedo, (d) number of clear looks

As a note, among all the kernels mentioned above, the most selected kernels in this map of New England are the RossThick kernel for the volumetric selection (99.7%) and the family of LiSparse-Reciprocal (97.7%) kernels for the geometric-optical selection. This is caused by the fact that the bidirectional geometry pattern of NOAA AVHRR data is similar across the scene and by the generally stable behavior of the RossThick-LiSparse reciprocal model (which is the simple model used in the current MODIS BRDF/albedo algorithm).

CONCLUSION

Currently and in the near future, global BRDF data will be collected from a number of remote sensing instruments with a wide field of view. The bidirectional reflectances are accumulated sequentially through daily observation in a given time period and the ground covers are assumed not to change during this period. If the effects of cloudiness are taken into account the number of usable bidirectional reflectances obtained in the period may be very limited. In the past, Wanner et al. (1995) used the minimal least squares best fit criteria to find the kernel combinations among a number of semiempirical kernels that best fit the data. Validation has produced good results. But when the sample size is limited the result is unstable and unreliable. It loses robustness especially when a small number of observations with large measurement errors occur in the data set. In this

paper, we calculated the variance of the albedo and found that the unreliable results are related to the occurrence of large variance in the derivation of the albedo. In these cases, the best fit method for selecting the kernels to employ may not yield the best result.

In order to obtain a more reliable inversion result, we introduced a new criteria which selects the kernel combinations which yield the least variance of albedo. The variance of white-sky albedo can be understood as being caused by the amplification of noise in the measurement and errors in the BRDF models. The least variance method always selects the kernels with the least noise sensitivity to the given observations. Tests show that the new method has a better capacity of interpolation and extrapolation and is more reliable with small sample sizes and less sensitive to the observation geometry. Therefore the new method of kernel selection would be suitable for small sample inversions. Furthermore, the variance map of albedo can help us to assess the inversion result and can help us to understand the product quality.

Note that the MODIS BRDF/Albedo algorithm (Lucht et al., 2000) uses only a single kernel combination as the BRDF model for inversions (the RossThick-LiSparse-Reciprocal model). In that case, least-squares and least variances inversions yield identical results. However, in a situation where the user is allowed to choose between multiple kernels, each suited specifically to a certain type of surface, the least variance method is the preferred method of inversion, as demonstrated in this paper.

The authors would like to thank Robert d'Entremont for providing the preprocessed bidirectional NOAA AVHRR data, Don Deering and Dan Kimes for allowing us to use their BRDF measurements. Thanks also to Xiaowen Li, Zong-Guo Xia and Jean Louis Roujean for useful discussions. This work was supported by NASA contract NAS5-31369.

REFERENCES

Acharya, P. K., Berk, A., Anderson, G.P., Larsen, N.F., Tsay, S-Chee, and Stamnes, K.H.(1999), MODTRAN4: Multiple Scattering and Bi-Directional Reflectance Distribution Function (BRDF) Upgrades to MODTRAN. Proc. of SPIE, Optical Spectroscopy Techniques and Instrumentation for Atmospheric and Space Research, 19-21 July 1999, Vol. 3756.

Barnsley, M. J., Strahler, A. H., Morris, K. P., and Muller J. P. (1994), Sampling the surface bidirectional reflectance distribution function (BRDF): 1. evaluation of current and future satellite sensors. *Remote Sens. Review.* 8:271-311.

d'Entremont, R. P., Schaaf, C. B., Lucht, W., and Strahler, A. H. (1999), Retrieval of red spectral albedo and bidirectional reflectance from 1-km² satellite observations for the New England region. *J. Geophys. Res.* 104:6229-6339.

Diner, D.J., Beckert, J.C., Reilly, T.H., Bruegge, C.J., Conel, J.E., Kahn, R.A., Martonchik, J.V., Ackerman, T.P., Davies, R., Gerstl, S.A.W., Gordon, H.R., Muller, J.-P., Myneni, R.B., Sellers, P.J., Pinty, B. and Verstraete, M.M. (1998) Multi-angle imaging spectroradiometer (MISR) instrument description and experiment overview. *IEEE Trans. Geosci. Remote Sens.*, 36:1072-1087.

Engelsen, O., Pinty, B., Verstraete, M. M., and Martonchik, J. V. (1996), Parametric bidirectional reflectance factor models: evaluation, improvements and applications, report, Joint Research Center of the European Commission, EU 16426, 114 pp.

Hu, B., Wanner, W., Li, X., and Strahler, A. H. (1997), Validation of kernel-driven semiempirical models for global modeling of bidirectional reflectance. *Remote Sens. Environ.* 62:201-214.

Justice, C.O., Vermote, E., Townshend, J.R.G., DeFries, R., Roy, D.P., Hall, D.K., Salomonson, V.V., Privette, J.L., Riggs, G., Strahler, A., Lucht, W., Myneni, R.B., Knyazikhin, Y., Running, S.W., Nemani, R.R., Wan, Z., Huete, A.R., van Leeuwen, W., Wolfe, R.E., Giglio, L., Muller, J.-P., Lewis, P. and Barnsley, M.J. (1998) The Moderate Resolution Imaging Spectroradiometer (MODIS): Land remote sensing for global change research. *IEEE Trans. Geosci. Remote Sens.*, 36:1228-1249.

Kimes, D. S. (1983), Dynamics of directional reflectance factor distribution for vegetation canopies. *Appl. Opt.* 22:1364-1372.

Leroy, M., Deuze, J. L., Breon, F. M., Hautecoeur, O., Herman, M., Buriez, J., Tanre, D., Bouffies, S., Chazette, P., and Roujean, J. L. (1997), Retrieval of atmosphere properties and surface bidirectional reflectance over land from POLDER ADEOS. *J. Geophys. Res.* 102:17023-17037.

Lewis, P., and Ruiz de Lope, E. V. (1997), Application of kernel-driven BRDF models and AVHRR data to monitoring land surface dynamics in the Sahel. *J. Remote Sens.* 1:155-161, 1997.

Lucht, W. (1998), Expected retrieval accuracies of bidirectional reflectance and albedo from EOS-MODIS and MISR angular sampling. *J. Geophys. Res.* 103:8763-8778.

Lucht, W., Schaaf, C.B., and Strahler, A.H. (2000), An algorithm for the retrieval of albedo from space using semiempirical BRDF models. *J. Geophys. Res.*, in press.

Privette, J. L., Eck, T. F., Deering, D. W. (1997), Estimating spectral albedo and nadir reflectance through inversion of simple BRDF models with AVHRR/MODIS-like data. *J. Geophys. Res.* 102: 29529-29542.

Roujean, J. L., Leroy, M., and Deschamps, P. Y. (1992), A bidirectional reflectance model of the Earth's surface for the correction of remote sensing data. *J. Geophys. Res.* 97:20455-20468.

Strahler, A. H., Wanner, W., Schaaf, C. B., Li, X., Hu, B., Muller, J. -P., Lewis, P., and Barnsley, M. J. (1996), *MODIS BRDF/Albedo product: Algorithm theoretical basis document*. NASA EOS MODIS Doc., version 4.0.

Tarantola, A. (1987), *Inverse problem theory: methods for data fitting and model parameter estimation*. Elsevier Science Publishing Company INC., New York.

Wanner, W., Li, X., and Strahler, A. H. (1995), On the derivation of kernels for kernel-driven models of bidirectional reflectance. *J. Geophys. Res.* 100:21077-21089.

Wanner, W., Strahler, A. H., Hu, B., Li, X., Schaaf, C. B., Lewis, P., Muller, J. -P., and Barnsley, M. J. (1997), Global retrieval of bidirectional reflectance and albedo over land from EOS MODIS and MISR data: Theory and algorithm. *J. Geophys. Res.* 102: 17143-17161.

Fig. 1 Test dataset (B)-(E) were deliberately selected from data set (A) and were prepared to be used in testing two inversion methods.

Fig. 2 Retrieved albedos may effect by the geometries of observations. Only 4 observations were used. For each land cover type, observations were randomly selected from the original data sets and retrieved. In the figures, albedos inverted by the best-fit method are more discrete than those by the least variance method. The best-fit method of kernel selection is therefore more sensitive to the bidirectional observation geometries.

Fig. 3 The accuracy of retrieved albedo may be effected by number of looks. In the figure, the least variance method is more stable than the best-fit method. (LV: the least variance method; LS: the best fit method)

Fig. 4 NIR waveband white-sky albedo of New England from NOAA AVHRR for a time period during September 1995. (a) is white-sky albedo produced by the least variance method. (b) is white-sky albedo produced by the best-fit method. (c) is standard deviation of white-sky albedo. (d) is numbers of clear looks. Black area in above maps are non-inverted pixels or water.

Table 1 Inverted results of two methods for five different land cover types in red band (A) and NIR band (B) (WSA: white-sky albedo; SD: standard deviation; SSE: sum square of errors; LV: least variance method; BF: best fitting method; ***: no result)

Group	Land cover	Field		Hardwood		Pine		Soybean		Grass	
		Methods	LV	BF	LV	BF	LV	BF	LV	BF	LV
A	WSA	0.2037	0.2248	0.0382	0.0363	0.0443	0.0415	0.0405	0.0368	0.3383	0.3260
	SD	0.0145	0.0201	0.0099	0.0101	0.0098	0.0099	0.0098	0.0102	0.0132	0.0133
	SSE	0.0165	0.0143	0.0119	0.0089	0.0301	0.0271	0.0138	0.0083	0.0334	0.0172
B	WSA	0.2802	-0.401	0.0360	0.0360	0.0378	0.0378	0.0367	0.0123	0.3056	-0.098
	SD	0.1628	10.536	0.1628	0.1628	0.1640	0.1640	0.1617	1.1149	0.1595	6.0035
	SSE	0.0001	0.0001	0.0001	0.0001	0.0000	0.0000	0.0000	0.0000	0.0001	0.0001
C	WSA	0.2334	0.0575	0.0317	0.0133	0.0374	0.0386	0.0361	0.0763	0.3466	0.3056
	SD	0.0895	0.6384	0.0895	0.6384	0.0821	0.1393	0.0924	0.4478	0.0946	0.1416
	SSE	0.0002	0.0001	0.0001	0.0001	0.0001	0.0001	0.0001	0.0000	0.0002	0.0001
D	WSA	0.2049	0.1913	0.0410	0.0531	0.0431	0.0387	0.0372	0.0437	0.3176	0.3068
	SD	0.0428	0.0444	0.0428	0.0670	0.0457	0.0505	0.0413	0.0544	0.0411	0.0424
	SSE	0.0007	0.0002	0.0002	0.0001	0.0001	0.0001	0.0001	0.0001	0.0023	0.0013
E	WSA	0.2354	***	0.0370	***	0.0443	***	0.0367	***	0.3599	***
	SD	0.0998	***	0.0998	***	0.1155	***	0.0687	***	0.0653	***
	SSE	0.0000	***	0.0000	***	0.0000	***	0.0000	***	0.0000	***

(A)

Group	Land cover	Field		Hardwood		Pine		Soybean		Grass	
		Methods	LV	BF	LV	BF	LV	BF	LV	BF	LV
A	WSA	0.2434	0.2686	0.3616	0.3602	0.2607	0.2579	0.5104	0.5042	0.4423	0.4277
	SD	0.0145	0.0201	0.0099	0.0101	0.0098	0.0099	0.0098	0.0101	0.0132	0.0133
	SSE	0.0244	0.0199	0.4494	0.4479	0.5641	0.4937	0.7053	0.6466	0.0601	0.0525
B	WSA	0.3408	-0.557	0.4385	-0.574	0.3419	1.8426	0.3356	-2.318	0.3955	0.3955
	SD	0.1628	10.536	0.1628	4.8633	0.1640	9.0143	0.1617	6.7225	0.1595	0.1595
	SSE	0.0001	0.0001	0.0009	0.0001	0.0002	0.0001	0.0011	0.0001	0.0001	0.0001
C	WSA	0.2757	0.1551	0.3718	-0.091	0.2873	0.2163	0.6462	0.4070	0.4648	0.3922
	SD	0.0895	0.4504	0.0895	0.9157	0.0821	0.1173	0.0924	0.1079	0.0946	0.1416
	SSE	0.0003	0.0001	0.0011	0.0002	0.0003	0.0002	0.0008	0.0004	0.0005	0.0001
D	WSA	0.2424	0.2264	0.3756	0.3692	0.2444	0.2586	0.5771	0.5744	0.4200	0.4067
	SD	0.0428	0.0444	0.0428	0.0448	0.0457	0.0695	0.0413	0.0427	0.0411	0.0424
	SSE	0.0012	0.0004	0.0007	0.0004	0.0001	0.0001	0.0005	0.0004	0.0010	0.0004
E	WSA	0.2818	***	0.3921	***	0.2237	***	0.5719	***	0.4785	***
	SD	0.0998	***	0.0998	***	0.1155	***	0.0687	***	0.0653	***
	SSE	0.0000	***	0.0000	***	0.0000	***	0.0000	***	0.0000	***

(B)

Table 2 Six land cover types selected for testing the capacities of interpolation and extrapolation (from PARABOLA data sets)

Land Cover Types	Number of SZA	SZA Range (degree)	LAI	red_WSA	Nir_WSA
Soil	5	21-62	<0.1	0.117	0.157
Grass	8	27-68	1.5	0.095	0.289
Cotton	6	37-65	4.0	0.035	0.630
Aspen	5	40-65	3.3	0.023	0.422
Black Spruce	7	35-65	6.3	0.030	0.164
Jack Pine	6	40-69	1.2	0.039	0.194

Table 3 Relative interpolated and extrapolated errors of black-sky albedo derived by the least variance and the best-fit method in red and NIR band.

	Red band black-sky albedo				NIR band black-sky albedo			
	Interpolation		Extrapolation		interpolation		Extrapolation	
	LV	BF	LV	BF	LV	BF	LV	BF
Grass	6.863	10.545	19.189	23.175	1.991	3.442	4.532	5.856
Soil	5.456	4.386	13.181	20.230	4.714	4.862	15.178	24.599
Cotton	5.397	5.435	5.006	5.123	0.963	7.019	2.897	6.627
Aspen	4.708	5.679	5.358	5.488	2.849	4.854	2.732	4.513
Black Spruce	6.693	9.213	7.618	8.621	2.669	2.678	7.617	4.414
Jack Pine	5.464	4.652	9.749	11.705	3.000	3.331	3.480	4.634
Average	5.764	6.652	10.017	12.390	2.698	4.364	6.073	8.441

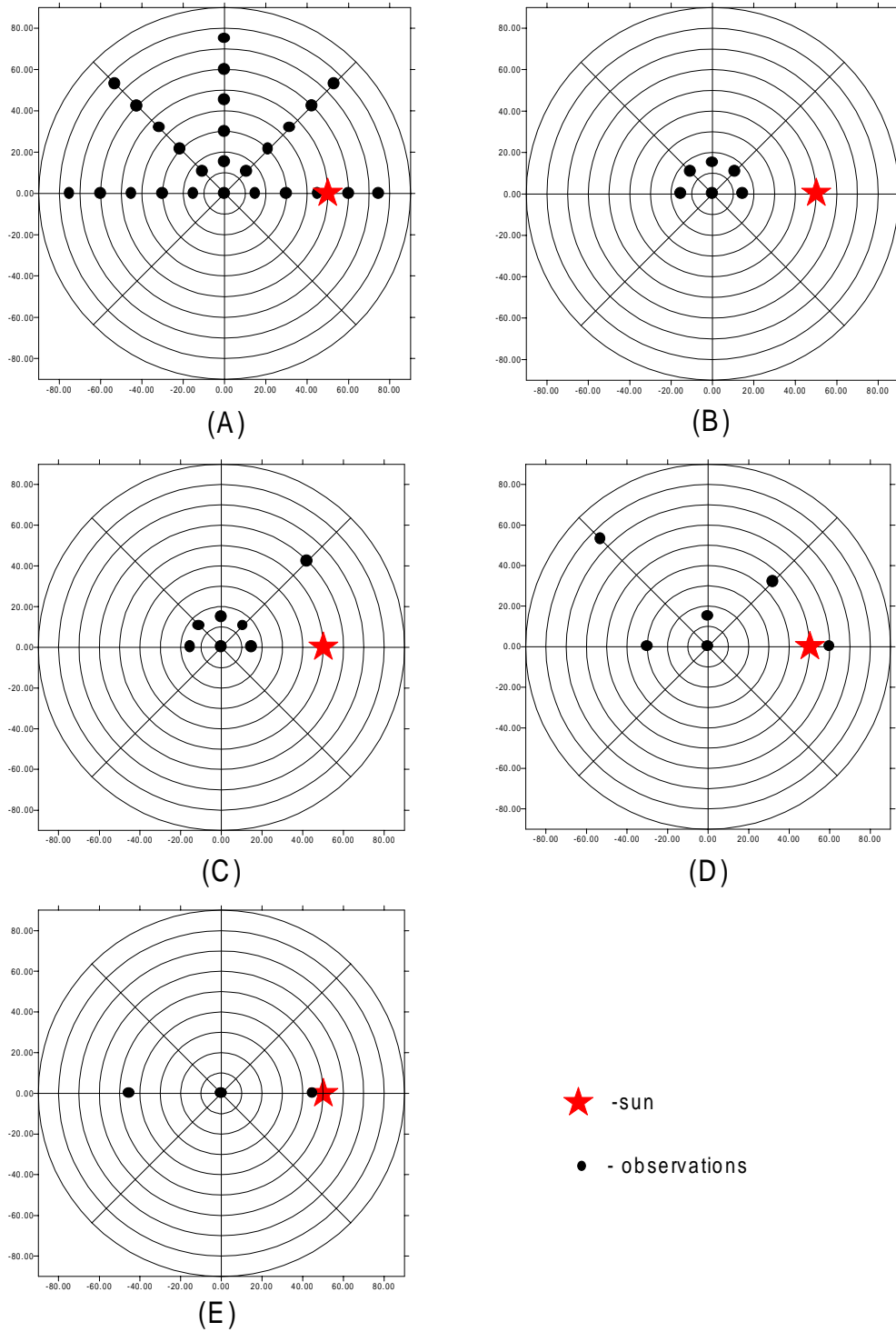
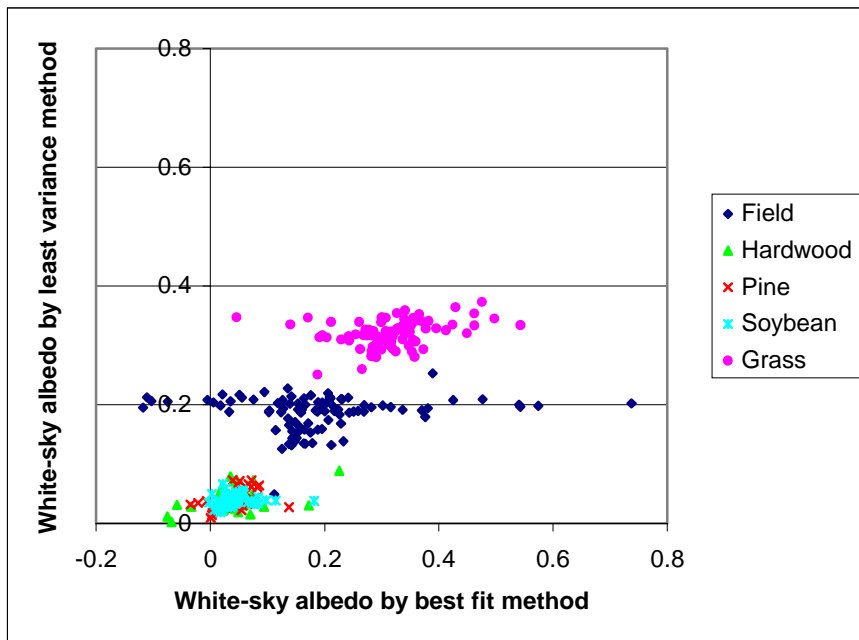
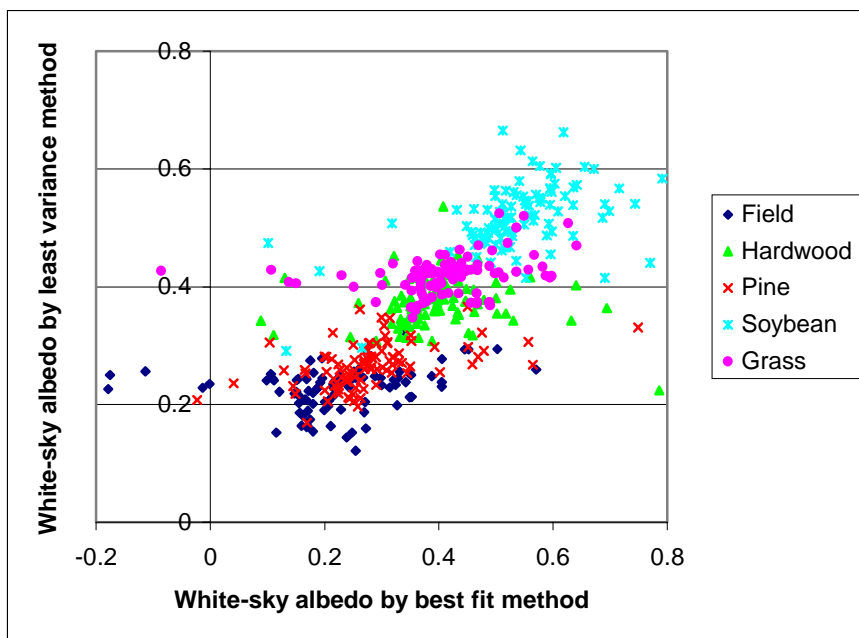


Fig. 1 Test dataset (B)-(E) were deliberately selected from data set (A) and were prepared to be used in testing two inversion methods.



(a) red band



(b) NIR band

Fig. 2 Retrieved albedos may effect by the geometries of observations. Only 4 observations were used. For each land cover type, observations were randomly selected from the original data sets and retrieved. In the figures, albedos inverted by the best-fit method are more discrete than those by the least variance method. The best-fit method of kernel selection is therefore more sensitive to the bidirectional observation geometries.

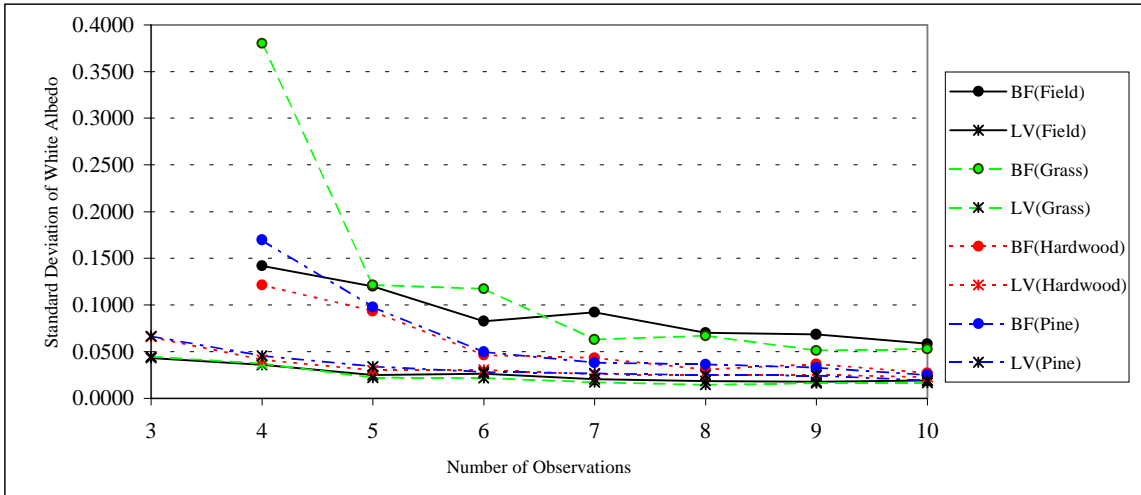


Fig. 3 The accuracy of retrieved albedo may be effected by number of looks. In the figure, the least variance method is more stable than the best-fit method. (LV: the least variance method; LS: the best fit method)

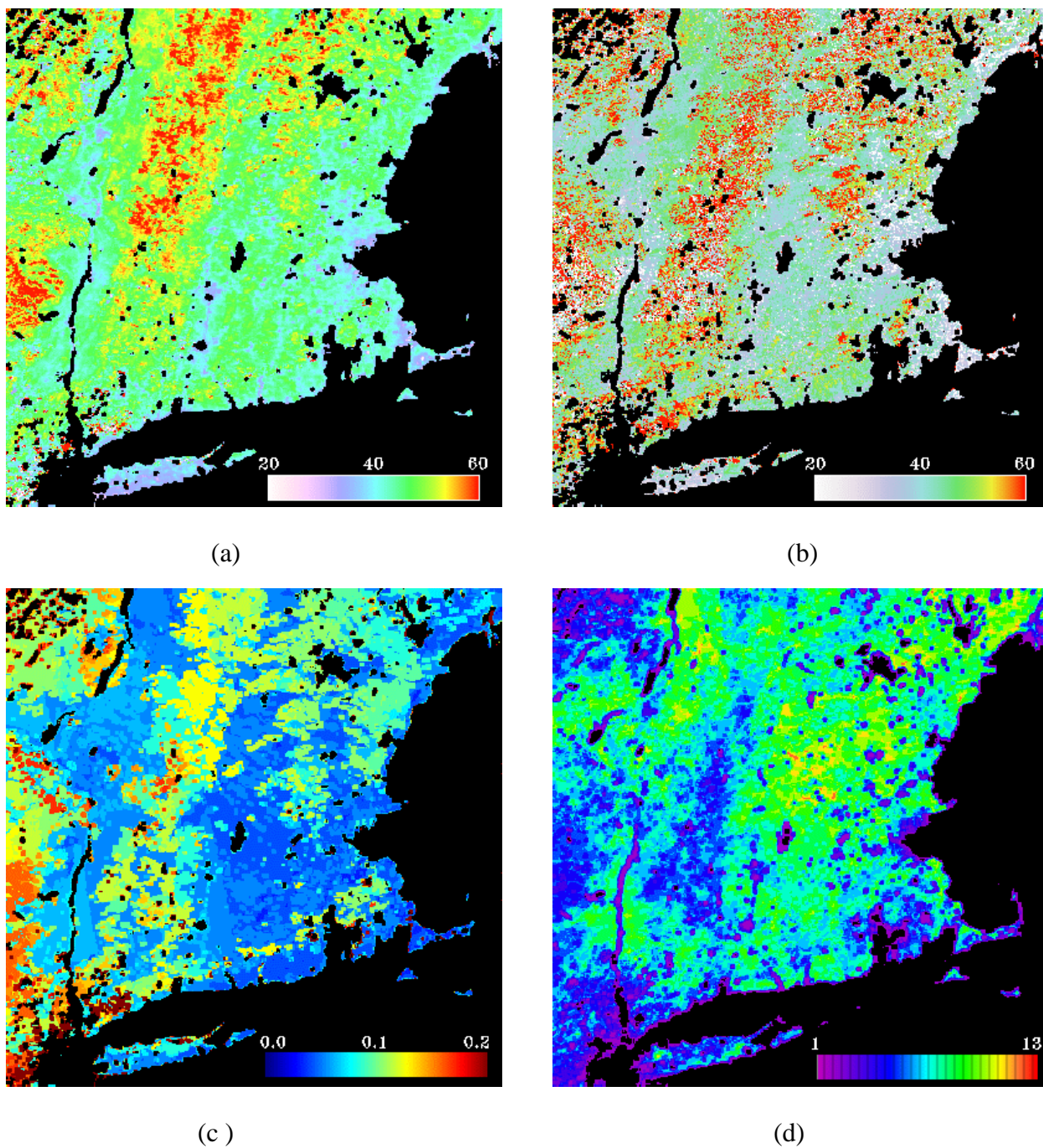


Fig. 4 NIR waveband white-sky albedo of New England from NOAA AVHRR for a time period during September 1995. (a) is white-sky albedo produced by the least variance method. (b) is white-sky albedo produced by the best-fit method. (c) is standard deviation of white-sky albedo. (d) is numbers of clear looks. Black area in above maps are non-inverted pixels or water.